LBNL-57385

CFD Investigation of Room Ventilation for Improved Operation of a Downdraft Table: Novel Concepts

Astrid H. Kristoffersen[1,2], Buvaneswari Jayaraman[1],
Elizabeth U. Finlayson[1], Ashok J. Gadgil[1]

[1]Indoor Environment Department
Environmental Energy Technologies Division
Lawrence Berkeley National Laboratory,
Berkeley, CA 94720, USA.

[2]Norwegian Building Research Institute
Forskningsvn.3b, 0314
Oslo, NORWAY

April 2005

This work was partly supported by the Norwegian Research Council through the Strategic Institute Program "Environmentally Favorable Energy Use in Buildings" at the Norwegian Building Research Institute, Project No. 133692/420; U.S.-Norway Fulbright Foundation for Educational Exchange and Lawrence Livermore National Laboratory, through the U.S. Department of Energy under Contract No. DE-AC03-76SF00098.

CFD Investigation of Room Ventilation for Improved Operation of a Downdraft Table: Novel Concepts

Astrid H. Kristoffersen[1,2], Buvaneswari Jayaraman[1], Elizabeth U. Finlayson[1], Ashok J. Gadgil[1]

[1]Indoor Environment Department, Lawrence Berkeley National Laboratory, Berkeley, CA 94720, USA.
[2]Norwegian Building Research Institute, Forskningsvn.3b, 0314 OSLO, NORWAY.
Email: astrid.kristoffersen@vetco.com

Summary: *We report a computational fluid dynamics (CFD) study of containment of airborne hazardous materials in a ventilated room containing a downdraft table. Specifically, we investigate the containment of hazardous airborne material obtainable under a range of ventilation configurations. The desirable ventilation configuration should ensure excellent containment of the hazardous material released from the workspace above the downdraft table. However, increased airflow raises operation costs, so the airflow should be as low as feasible without compromising containment. The airflow is modeled using Reynolds Averaged Navier Stokes equations with a high Reynolds number k-epsilon turbulence model. CFD predictions are examined for several ventilation configurations. Based on this study, we find that substantial improvements in containment are possible concurrent with reduction in airflow, compared to the existing design of ventilation configuration.*

Keywords: *CFD modeling, downdraft table, ventilation, contamination control.*

INTRODUCTION

Downdraft tables are used to handle hazardous materials that can become airborne. The ventilation configuration in the room containing the downdraft table affects the downdraft table performance. Experimental work on a downdraft table has been reported [1], however no published guidelines are available in the literature for room ventilation design to improve the performance of an industrial downdraft table. Although numerical and experimental work has been published investigating the performance of fume hoods (e.g. ref [2]), fume hoods are unsuitable where manipulating operations are required. The present study investigates possible modifications to the ventilation system of a downdraft facility using computational fluid dynamics (CFD). Some of our work on this facility has been reported in [3], [4].

The objective of this study is to improve containment of the contaminant by changing the ventilation configuration. Energy costs can be reduced if improved containment can be achieved with reduced airflow. The facility under investigation remains contaminated from previous use and is inaccessible for detailed experiments. Therefore, any assessment of improving containment and reducing airflow must be undertaken with simulations. The present study uses CFD to test alternate ventilation and geometric configurations for improved containment of the pollutants.

FACILITY AND MODEL DESCRIPTION

The facility, shown schematically in Fig. 1, consists of two rooms connected by a doorway. In the first room, the change room, the worker puts on protective clothing. This room provides an entrance to the second room, the downdraft room (2.3m x 2.0m x 2.5m high), which contains the downdraft table located against the wall opposite to the door. This wall has in it a pass-through window directly above the downdraft table. After the contaminated packages are passed into the room through this window, the window is closed. As the facility is currently operated, air enters the room through a vertical slot in the door behind the worker, and from a rectangular inlet in the ceiling above the table. All airflow exits through the downdraft table. The rooms, constructed in the 1960s, currently have a ventilation configuration that supplies a total of 1700 l/s (3600 cfm) air to the room. Of this 1230 l/s (2600 cfm) are supplied through an opening in the door connecting the two rooms and 470 l/s (1000 cfm) from the ceiling towards the table. The vertical slot in the door has dimension 0.46 m x 0.81 m (18" x 32"), with its lower edge located at 10 cm (4 inches) from the floor level. This opening in the door is referred to as the door inlet.

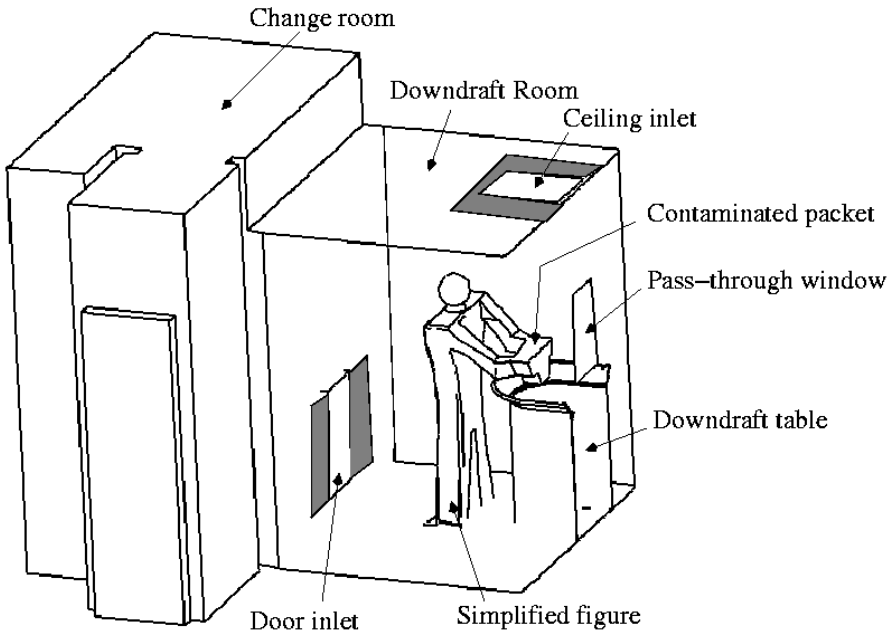

FIGURE 1. Facility geometry including the change room to the left and the downdraft room to the right (2.3m x 2.0m x 2.5m). The geometry includes the downdraft table, simplified worker figure in a protective suit holding the contaminated package, door inlets, pass-through window, and an inlet in the ceiling

The change room was excluded from the computational domain. When the door is closed the details of the airflow within the change room were assumed to have no effect on the airflow in the downdraft room. Airflow enters the downdraft room through the door slot, normal to the door, and was treated as a boundary condition. The airflow from the inlet in the ceiling was assumed to be straight down, and also treated as a boundary condition. Additional inlets for

alternate configurations were all treated as boundary conditions. Inlet boundary conditions had specified flow rates.

A simplified model of a worker simulated the effect of flow blockage by the worker. The worker is assumed to be in a protective suit and the thermal plume of the worker is neglected (owing to larger than an order of magnitude difference between the plume velocity in still air, and the downdraft room airspeeds). The worker is holding an object representing a contaminated package. The package is held above the downdraft table surface and away from the edge in order to represent standard working conditions.

Containment for a given velocity field was investigated by first checking the predicted flow paths of massless particles, and then, in more detail, checking the predicted concentration of tracer gas. The massless particles and the tracer gas were both released from the package and the two additional locations where "worst-case" containment was expected: from the rim of the downdraft table, and the perimeter of the (closed) window in the wall behind the downdraft table (Figure 2). Tracks of airborne massless particles give a good indication of whether contaminant will be contained with respect to the mean flow. This is a reasonable minimum criterion to assure containment. Particle tracks can show the effects only of the mean velocity. Additional mixing in the room from turbulent fluctuations can cause increased contamination. To evaluate the additional diffusion caused by turbulence, we simulated a continuous release of a neutrally buoyant tracer gas (as a passive scalar) at the rim of the downdraft tabletop and the perimeter of the pass-through window. Tracer gas has very high diffusivity, much larger than that of particulate contaminants, and represents a maximum criterion for containment of particles.

We considered several modifications to the existing room operation and geometry, by changing the area, location and airflow from the inlets. One configuration also investigated the performance with a perforated floor as exhaust, and perforated ceiling as inlet.

We performed the CFD calculations using the Reynolds Averaged form of the Navier Stokes Equations (RANS). The flow is considered incompressible and isothermal with constant air properties. The standard k-ε turbulence model (Eq. 3,4) is used. A finite volume formulation of the following set of equations is solved using the commercial software Star-CD [5].

$$\frac{\partial \mathrm{U_j}}{\partial \mathrm{x_j}} = 0 \tag{1}$$

$$U_j \frac{\partial U_i}{\partial x_j} = -\frac{1}{\rho}\frac{\partial P}{\partial x_i} + \frac{\partial}{\partial x_j}\left(\nu \frac{\partial U_i}{\partial x_j}\right) - \frac{2}{3}\frac{\partial k}{\partial x_i} \tag{2}$$

$$\mathrm{U_j}\frac{\partial \mathrm{k}}{\partial \mathrm{x_j}} = \frac{\partial}{\partial \mathrm{x_j}}\left(\nu \frac{\partial \mathrm{k}}{\partial \mathrm{x_j}}\right) + \nu_{\mathrm{turb}}\left(\frac{\partial \mathrm{U_i}}{\partial \mathrm{x_j}} + \frac{\partial \mathrm{U_j}}{\partial \mathrm{x_i}}\right)\frac{\partial \mathrm{U_i}}{\partial \mathrm{x_j}} - \varepsilon \tag{3}$$

$$U_j \frac{\partial \varepsilon}{\partial x_j} = \frac{\partial}{\partial x_j}\left(\nu_{molec} + \frac{\nu_{turb}}{1.22}\frac{\partial \varepsilon}{\partial x_j}\right) + \frac{\varepsilon}{k}\left[1.44 \upsilon_{turb}\left(\frac{\partial U_i}{\partial x_j} + \frac{\partial U_j}{\partial x_i}\right)\frac{\partial U_i}{\partial x_j}\right] - 1.92\frac{\varepsilon^2}{k} \tag{4}$$

$$\mathrm{U_j}\frac{\partial C}{\partial x_j} = \frac{\partial}{\partial x_j}\left(D_{molec} + \frac{\nu_{turb}}{\sigma_m}\right)\frac{\partial C}{\partial x_j} \tag{5}$$

where: P is the pressure; ρ is the density; U_i are the mean velocity components; x_i are rectilinear orthogonal coordinates; k is the turbulent kinetic energy; ε is the dissipation rate of k; C is the tracer concentration, $\nu = \nu_{turb} + \nu_{molec}$ where ν_{molec} is the molecular kinematic viscosity and ν_{turb} is the turbulent kinematic viscosity: $\nu_{turb} = 0.09k^2\varepsilon^{-1}$. D_{molec} is the molecular diffusivity of air in air and σ_m is the turbulent Schmidt number, assigned a value of 0.6.

We have earlier demonstrated very good agreement between CFD predictions of room mixing time and experiments [6]. Our recent research [7] shows that a RANS model with a second-order differencing scheme that suppresses numerical diffusion can provide acceptable (i.e., within a factor of two compared to experimental measurements) detailed predictions for pollutant dispersion. Justification for our current approach rests on the successful CFD comparison to experiment reported in [7]. Another way of examining the containment would be to perform a Large Eddy Simulation (LES) and actually calculate the turbulent eddies. A Large Eddy Simulation (LES) would have increased the computational and human effort significantly.

Equations for the airflow were first solved to obtain a steady state velocity field in the downdraft room using the SIMPLE algorithm [8], and a second-order differencing scheme. The tracer gas transport equation was solved by taking this airflow field as given and treating the tracer gas as a neutrally buoyant and non-reacting scalar. Examination of the simulated tracer gas concentration throughout the downdraft room gave an indication of the spread of the tracer gas due to turbulent diffusion. Mass conservation of the air is fulfilled by specifying as boundary conditions that same amount of air enters the room leaves the room. The computational grid consists of approximately 670,000 nodes. The grid was locally refined until less than 10% changes were recorded in the overall mean velocities, max and min velocities, and pressure.

The steady state airflow calculations were terminated when the normalized sum of the residuals decrease to less than 1.0e-4. The tracer dispersion was calculated for this airflow field. The calculations for the steady state solution of the tracer were terminated when the normalized sum of the residual became less than 5.0e-5. The mass conservation of tracer gas was checked and found to be within 1%, for all simulated cases.

Since the tracer gas responds to the turbulent diffusion just as much as air, its release provides an estimate of dispersion and containment of species with high diffusivity. Particles have lower diffusivity than tracer gas, so, particles released at the same locations and with the same velocity, will diffuse less and thus can be expected to be better contained than tracer gas.

Particles can be released with an initial velocity owing to small mechanical energy being imparted to them. In that case, the particles will initiate their travel with some momentum, and may not follow the streamlines. We demonstrate below that this is not a cause for concern.

Mechanically generated powder constituents are typically larger than about 10 microns. For a given launch velocity, larger particles travel farther before coming to momentum equilibrium with the surrounding air. The time for reaching equilibrium is called the relaxation time. Consider a 100 micron particle released from the contaminated packet 4 inches from the rim of the downdraft table, towards the rim. The relaxation time for a 100 micron particle is 3.1×10^{-2} sec [9]. A launch velocity of more than 3.2 m/s (630 ft/min) would be required for the particle to reach the rim. For a 10 micron particle the velocity would be two orders of magnitude higher. Since the downdraft table is not used for explosive releases, we do not anticipate particles leaving the package at velocities high enough to reach the rim.

Figures 3 and 4 show the section planes that will be used to display the results.

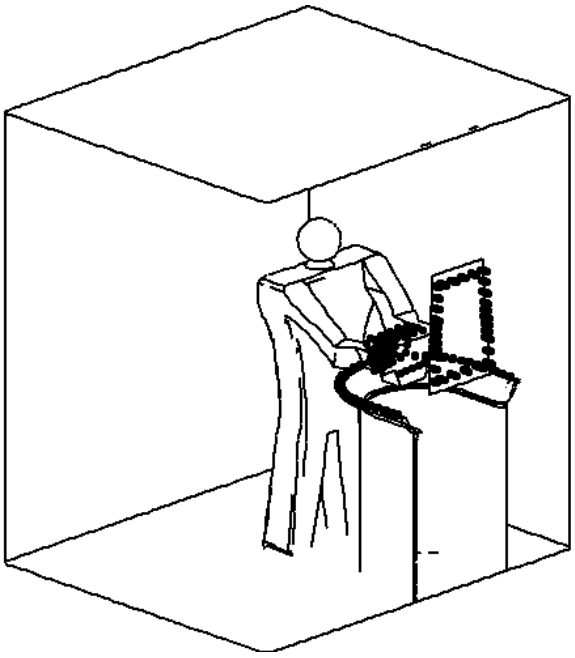

FIGURE 2. Simulated release of massless particles and tracer gas used to determine containment. Release locations are shown as black spots

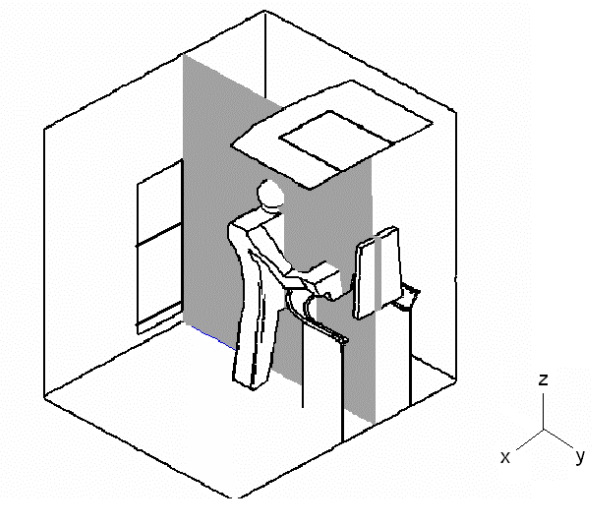

FIGURE 3. The Y-Z section used for displaying results in subsequent figures. The plane passes through the middle of the human figure showing the asymmetry of the downdraft table position within the room. Center plane of downdraft table is 33”(0.84m) from the left wall and 56”(1.42m) from the right wall. This section illustrates the containment in front of the worker, and around the package. Note that the display plane cuts through the torso of the figure and misses either of the legs. Hence legs appear missing in this view in Figures 6-9.

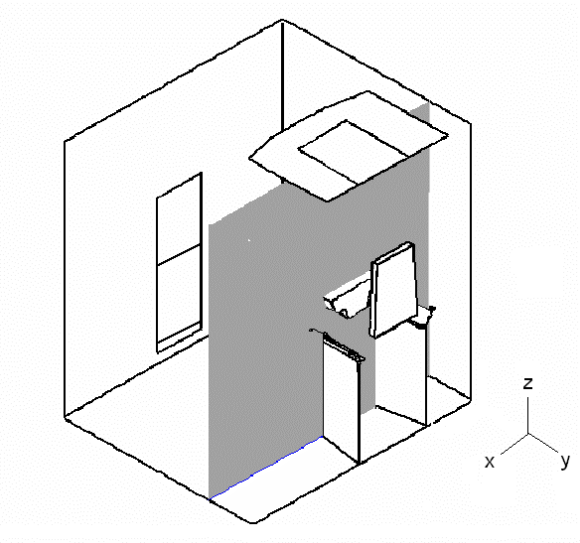

FIGURE 4. The X-Z section used for displaying results in subsequent figures. The plane cuts through the middle of the contaminated package. This view shows how the contamination is spread into the room on either side of the table.

We now introduce a measure of the contamination spill, S, in the room. The spill is calculated throughout the computational domain excluding the cells inside the downdraft table, and the cells where the tracer gas is released. For a small release rate of tracer the spill was defined as the integral of the tracer-concentration-weighted cell volumes divided by the same volume, normalized by the concentration at the exhaust. If the release rate of tracer is X kg/s and the fresh air-supply rate is M kg/s and X << M, then we can write

$$S = \frac{\int CdV}{\int dV} \frac{M}{X} \tag{6}$$

Mass balance requires that, the concentration at the exhaust must be X/(X + M) at steady state. In an instantaneously perfectly mixed room, the tracer gas concentration in the room will be the same as the concentration at the exhaust. Therefore, for an instantaneously perfectly mixed room C = X/(X + M). When X << M, then C = X/M and the spill measure S = X/M*M/X = 1. If the contaminants are fully contained into the downdraft table S=0, and there is no spill. The spill measure gives a measure of the average concentration of the tracer in the room, in the steady state, and is normalized to be between 1 (max) and 0 (min). So for a given spill measure, S, the average pollutant concentration in the downdraft room, outside of the downdraft table, is obtained by multiplying the exhaust concentration of the pollutant by the spill measure.

$$\text{Average concentration of pollutant in the downdraft room} = S * \frac{X}{M} \tag{7}$$

Description of the Different Configurations

The description of the different geometries is shown in Table 1.

Table 1. Definitions of inlet geometries

Inlet type	**Description**	**Area** m^2 (in^2)
Ceiling inlet	Existing	0.32 (500)
	Large	1.07 (1659)
	Perforated	4.42 (6843)
Door inlet	Existing	0.37 (576)
	Large	0.59 (911)
Side	Left	0.65 (1000)
	Right	0.65 (1000)
AirVest		0.17 (260)

The existing ceiling inlet is shown in Figure 1 as the non-shaded inlet in the ceiling (51 cm (20 inch) wide and 64 cm (25 inch) long). The large ceiling inlet includes the shaded area in the ceiling in Figure 1 (125 cm (49 inch) wide, and 86 cm (34 inch) long). The perforated ceiling inlet assumes that the entire ceiling is a perforated plate, and acts as an inlet. The perforated ceiling inlet is modeled with a perforated full-floor exhaust. The existing door inlet is shown as the non-shaded inlet behind the worker [46 cm (18 inches) wide and 81 cm (32 inches) high]. The large door inlet includes the shaded area on the left and right side of the existing door inlet (72 cm (28.5 inches) wide and 81 cm (32 inches) high). If one draws a vertical plane similar to the one identified on Figure 3, the left edge of the large door inlet behind the worker will be coplanar with the left edge of the large ceiling inlet. The side inlets are positioned on the walls on the left and right side of the downdraft table. The "left inlet" is on the left hand side wall of the worker, and the "right inlet" on the right hand side wall of the worker. The low edge of the side inlets are 77 cm (30 inch) from the floor level; each inlet is 1 m (39 inch) long and 65 cm (26 inch) high, and its vertical edge nearest to the wall with the pass-through window is 30 cm (12 inch) from that wall.

The airvest is a device that could be worn by the worker, covering the worker's chest. The airvest could also be a device positioned in front of the downdraft table at the height of the worker's chest. The worker should then position himself behind the airvest when opening the packet. For previous research on reducing worker exposure using an airvest, see [10].

Table 2 lists the different geometrical configurations.

TABLE 2. Summary of different geometry configurations investigated

Config-urations	Ceiling inlet	Door inlet	Floor outlet	AirVest	Side flow
A	Existing	Existing	None	None	None
B	Large	Existing	None	None	None
C	Large	Large	None	None	None
D	Perforated	None	Perforated	None	None
E	Existing	Existing	None	Yes	Right and left

RESULTS

Discussion of Existing Configuration

As a first step we explored the containment capability of the existing configuration (Configuration A) as it is currently operating; 470 l/s (1000 cfm) downward from the ceiling inlet and 1230 l/s (2600 cfm) through the door.

Figure 6 shows the tracer concentration contours and velocity pattern for the existing configuration. All concentration contours presented in this paper are in log scale. In the y-z view, the spilled tracer touches the worker's chest and spreads into the room. In the x-z view, the tracer is spread on both sides of the table. A recirculating airflow pattern can be seen on the left hand side of the table in the x-z view. The airflow from the door inlet encounters either lower part of the downdraft table, or the opposite wall. The part of the airflow that rises along the wall (not seen in Figure 6) produces a recirculating flow in the room. The tracer reaches this recirculating pattern by turbulent diffusion, and becomes effectively spread in the room by following the mean flow recirulation. The contamination spill for the existing configuration was found to be $S = 8.64 \cdot 10^{-4}$.

The containment of the tracer gas is significantly increased when releasing tracer gas inside the downdraft table rather than releasing it from the rim and around the pass-through window. The spill measure for this release was measured to $S = 0.75 \cdot 10^{-4}$. It is recommended to open the packet inside a ring 10 cm (4 inch) from the downdraft table rim.

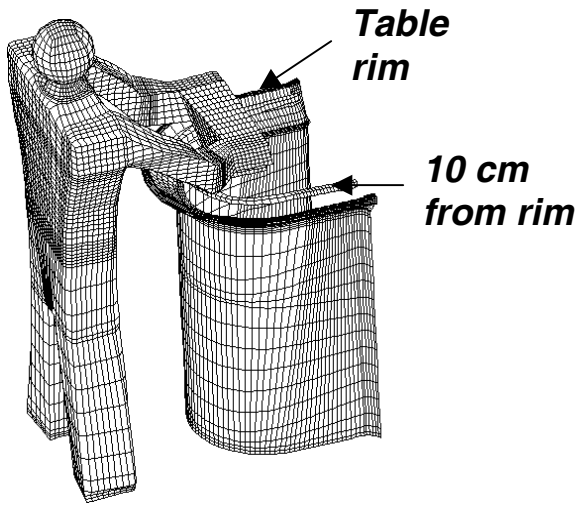

FIGURE 5. Tracer gas release locations 10 cm from the table rim, in the plane of the table rim

The existing configuration produced a recirculating pattern on the left hand side of the table in the x-z view. 18 different simulations with the same configuration, but reduced airflow were performed, varying the airflow from the ceiling inlet from 190 to 470 l/s (400 to 1000 cfm), and varying the airflow from the door inlet from 190 to 1220 l/s (400 to 2600 cfm). Results from previous work on this facility show that decreasing the airflow with the same geometry as the existing set up will reduce the contamination of the room [3]. The smallest spill measure among these 18 simulations was found for airflow from the ceiling inlet 380 l/s (800 cfm) and airflow from the door inlet 760 l/s (1600 cfm). The tracer concentration for configuration A with the "best" reduced airflow settings was found at 380 l/s (800 cfm) from the ceiling inlet and 760 l/s

(1600 cfm) from the door inlet. The spill measure was calculated to $S = 4.36 \cdot 10^{-4}$, a reduction of 50 % compared to the existing airflows. The spill is still high, because of the recirculating pattern that is still present. We now want to investigate other configurations to see if the recirculating pattern can be suppressed, and hence further reduce the spill measure.

Alternate Configurations

Configuration B has enlarged ceiling inlet, and existing door inlet. 19 different runs varying the airflow at the inlets have been performed. The case with the lowest spill measure has airflow from the ceiling inlet of 470 l/s (1000 cfm) and from the door inlet 380 l/s (800 cfm). The enlarged ceiling inlet reduces the extent of the recirculating flow seen in the x-z view of the velocity. This case further reduces the spill by about a factor of two giving a spill measure of $S = 2.42 \cdot 10^{-4}$. The tracer escapes from the downdraft table and enters the recirculating flow, contaminating the left side of the downdraft table.

Configuration C has the same ceiling inlet as configuration B, but also has an enlarged door inlet. The velocity and tracer concentration is shown in Figure 7. Configuration C suppresses the recirculating flow further, but is still present. The spill measure is further slightly reduced to $S = 2.22 \cdot 10^{-4}$.

Configuration D is successful in suppressing the recirculating pattern on the left side of the downdraft table. Airflow of 800 l/s (1700 cfm) is injected uniformly from the ceiling, resulting in vertically downward airflow from the ceiling. Part of the air leaves the room through a perforated floor, and the rest leaves through the downdraft table. Three simulations with this configuration were performed, with 10, 20 and 30% of the flow leaving the room through the perforated floor. Part of the airflow from the ceiling directly enters into the downdraft table, while the rest proceeds towards the floor mostly besides and behind the worker. A part of this airflow exits the room through the perforated floor, but the rest rises in front of the worker and is then sucked into the downdraft table. Very low velocities (~0.1 m/s) result in the region in front of the worker, where the rising air meets the downward airflow from the ceiling. The tracer gas transported by turbulent diffusion into this region contaminates the area around the downdraft table and in front of the worker. Forcing a larger part of the air to exhaust through the floor would prevent the air from rising when hitting the floor. Due to the size and geometry of this room, about 70% of supplied air must exhaust through the floor to prevent the rising airflow in front of the worker. The average air speed at the downdraft table face must exceed the recommended value of 200 ft. per min. [11], so the minimum acceptable flow to exit through the downdraft table is 560 l/s (1200 cfm). Having 560 l/s (1200 cfm) leaving the room through the downdraft table, and 70% of the injected air leaving the room through the floor, means that a total airflow of about 1880 l/s (4000 cfm) must be injected from the perforated ceiling. A total airflow of 1880 l/s (4000 cfm) is considered too high, so a different configuration is more appropriate.

Configuration E has ceiling inlet and door flow inlet as the original case, but adds three other inlets. The airvest is a lightweight vest worn by the worker that ejects low-velocity air from the chest region of the worker, away from the worker's body [10]. The airvest blows air from the chest of the worker towards the downdraft table in the horizontal direction. Fresh air from the chest of the worker prevents contaminated air from diffusing into his breathing zone. In addition, two large area, low velocity side inlets are positioned at either side of the downdraft table. The supply from the side inlets has low velocity resulting in a slow steady flow towards the downdraft table with low turbulent kinetic energy. The airflows from the different inlets are adjusted, so the

released particles are contained into the downdraft table, and not spread into the room. The optimal airflow rates were found to be: 70 l/s (150 cfm) from the airvest, 380 l/s (800 cfm) from the ceiling inlet, 280 l/s (600 cfm) from the door inlet, 380 l/s (800 cfm) from the left side inlet and 140 l/s (300 cfm) from the right side inlet. 15 different runs varying the airflow rates were performed with this configuration. A slow flow toward the downdraft table from inlets surrounding the downdraft table, leads to increased containment.

A few simulations were also performed with narrower side inlets. These simulations predicted significant spill. Only when the side inlets had large area and the airflow velocities small, we could see a significant reduction in the spill measure. The spill measure is reduced from $S = 8.64 \cdot 10^{-4}$ for the existing case to $S = 1.58 \cdot 10^{-4}$ for configuration E– a reduction of 82 %. The airflow is reduced by 26 %. The tracer concentration and velocities for Configuration E can be seen in Figure 8. The turbulent energy is also low for this configuration, as seen in Figure 9. The turbulent intensity is highest in the room at the rim of the table. The high turbulent intensity at the rim leads to high turbulent diffusivity, which leads to diffusive escape of some amount (though small) of the tracer gas from the rim into the room.

A simulation adding the airvest (without side inlets) to configuration A was also performed (not reported). This resulted in approximately the same result as configuration A, except that the area between the worker and the downdraft table was not contaminated due to the injection of fresh air from the airvest. Thus, the worker's exposure would indeed be reduced without noticeably reducing the spill measure.

The tracer concentration for a release of tracer gas from 10 cm (4 inch) inwards from the downdraft table rim for configuration E resulted in a spill measure of $S = 0.59 \cdot 10^{-4}$, a reduction of 21 % compared to the existing configuration. Opening the packet inside a ring of 10 cm (4 inch) inside the downdraft table is highly recommended.

The best run (based on calculation of the spill measure) of each configuration is listed in Table 3.

Table 3. Spill measure for the existing configuration and the best case for each configuration

Config-uration	Ceiling inlet l/s (cfm)	Door inlet l/s (cfm)	Floor outlet l/s (cfm)	AirVest l/s (cfm)	Left side inlet l/s (cfm)	Right side inlet l/s (cfm)	Total Airflow l/s (cfm)	Spill Measure 10^{-4}
Existing	470 (1000)	1220 (2600)	N/A	N/A	N/A	N/A	1690 (3600)	8.64
A	380 (800)	760 (1600)	N/A	N/A	N/A	N/A	1140 (2400)	4.36
B	470 (1000)	380 (800)	N/A	N/A	N/A	N/A	850 (1800)	2.42
C	470 (1000)	470 (1000)	N/A	N/A	N/A	N/A	940 (2000)	2.22
D	800 (1700)	None	240 (510)	N/A	N/A	N/A	800 (1700)	2.32
E	380 (800)	280 (600)	N/A	70 (150)	380 (800)	140 (300)	1250 (2650)	1.58

CONCLUSION

Despite the industrial wide scale use of down draft table, published literature does not provide guidelines or measures of how well a downdraft table performs under specific ventilation configurations in the room in which it is operated.

This paper defines a dimensionless "spill measure," that provides a quantitative measure of pollutant containment for a downdraft table operated under specific ventilation conditions. The spill measure has a maximum possible value of 1, and a minimum possible value of 0. In the steady state, the average concentration of the pollutant in the room is given by multiplying spill measure by the pollutant concentration in the exhaust from the room (or by weighted average pollutant concentration in the exhaust, if the room has multiple exhausts).

We examined the down draft table performance using CFD simulations, verified with earlier published comparison with different experiments. We showed that reducing the airflow supply in the existing geometric configuration would reduce the spill measure, and even the concentration of pollutant in the room (the reduction in the spill measure is larger than the increase in the pollutant concentration in the exhaust arising from reduction in the fresh air supply to the room). We also showed that even more reduction in the spill measure, and improved containment, are possible with increasing the area of inlets in the ceiling and the door with appropriate changes in the respective airflow supply rates, or with using a perforated ceiling air supply and a perforated floor exhaust. Finally, we showed that using two side-wall mounted air supplies and an airvest, the spill measure could be reduced even further, by more than a factor of 5 compared to the original configuration -- thus saving conditioning energy for the air supply (26%), and concurrently improving the containment of the contaminant and hence the worker protection (82%).

ACKNOWLEDGEMENT

This work was partly supported by: (1) The Norwegian Research Council through the Strategic Institute Program “Environmentally Favorable Energy Use in Buildings” at the Norwegian Building Research Institute, Project No. 133692/420; U.S.- Norway Fulbright Foundation for Educational Exchange; and (2) Lawrence Livermore National Laboratory and performed for the U.S. Department of Energy under Contract No. DE-AC03-76SF00098, at Lawrence Berkeley National Laboratory.

REFERENCES

1. **Spencer, A.B., C.F. Estill, J.B. McCammon, R.L. Mickelsen and O.E. Johnston:** Control of ethyl methacrylate exposures during the application of artificial fingernails. *Amer. Industrial Hygiene Assoc.* 58(3) pp. 214-218 (1997).

2. **Lan, N.S., and S. Viswanathan**: Numerical simulation of airflow around a variable volume/constant face velocity fume cupboard. *Amer. Industrial Hygiene Assoc.* 62(3) pp. 303-31 (2001).

3. **Finlayson, E.U., B. Jayaraman, A. Kristoffersen and A. Gadgil**: CFD analysis of LLNL downdraft table. *LBNL Report 53883.* (2003).

4. **Jayaraman, B., A.R. Kristoffersen, E. Finlayson and A. Gadgil**: Investigation of room ventilation for improved operation of a downdraft table. *LBNL Report 55561*, *Submitted to Indoor Air (2005).*

5. **Star-CD Version 3.15 Methodology**: *Adapco*. (2001).

6. **Gadgil A.J., C. Lobscheid, M.O. Abadie and E. U. Finlayson**: Indoor pollutant mixing time in an isothermal closed room: An investigation using CFD, *Atmospheric Environment* 37:5577-5586 (2003).

7. **Finlayson, E.U., A. J. Gadgil, T. L. Thatcher and R. G. Sextro**: Pollutant dispersion in a large indoor space: Computational Fluid Dynamics (CFD) predictions and comparison with a scale model experiment for isothermal flow, *Indoor Air* 14(4): 272-283 (2004).

8. **Patankar, S.V.**: *Numerical heat Transfer and Fluid Flow*, Hemisphere: Washington D.C., 1980.

9. **Hinds, W. C.**: Aerosol *Technology: Properties, Behavior, and Measurement of Airborne Particles.* John Wiley & Sons, 1999.

10. **Gadgil, A. J., D. Faulkner, W. J. Fisk**: Reduced worker exposure and improved energy efficiency in industrial fume hoods using an airvest, *Lawrence Berkeley National Laboratory Report LBNL-32244* (1992).

11. **ACGIH:** *Industrial Ventilation. A Manual of Recommended Practice 22nd Edition.* American Conference of Governmental Industrial Hygenists, 1995.

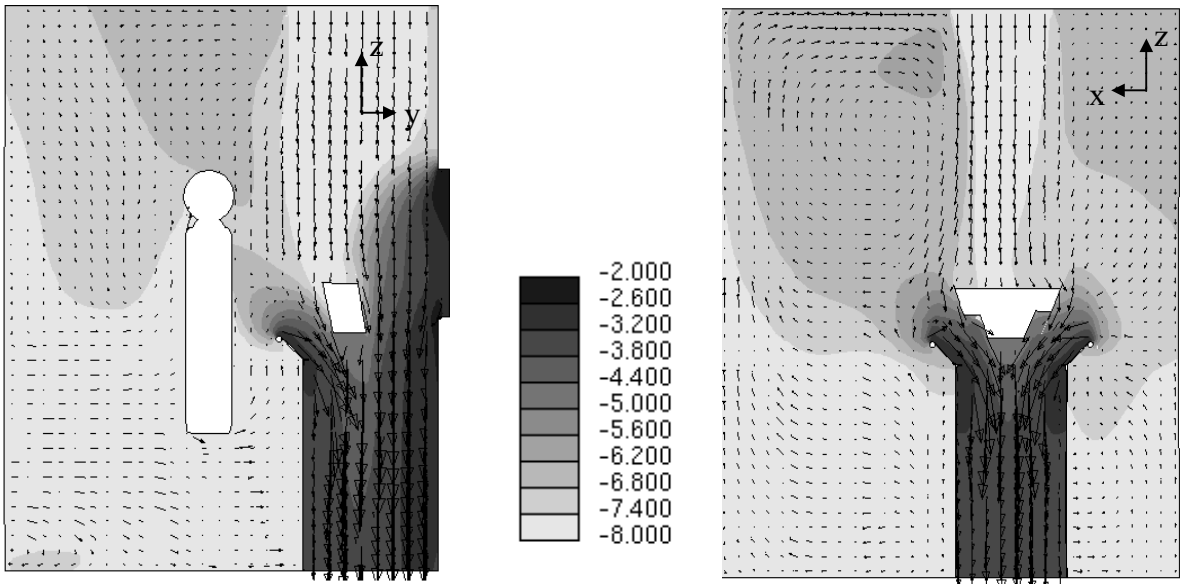

FIGURE 6. Tracer gas concentration (log of normalized concentration) and velocity of existing geometry with currently operated airflow rates: 470 l/s (1000 cfm) from the ceiling inlet and 1220 l/s (2600 cfm) from the door inlet, when releasing 1 g/s of tracer into the room.

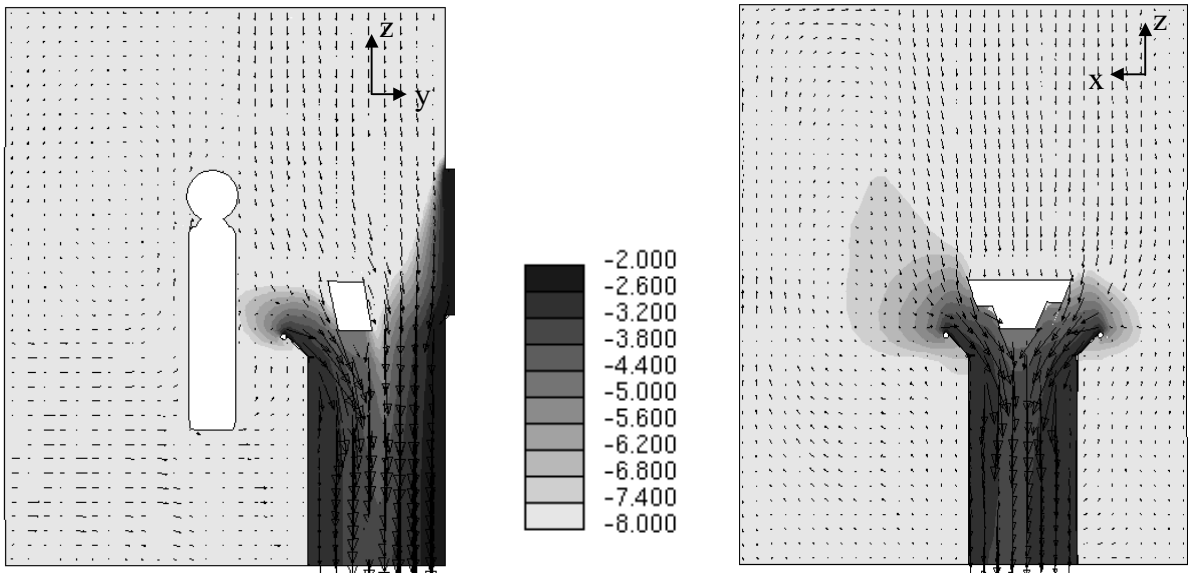

FIGURE 7. Velocity and tracer concentration with release of 1 g/s of tracer, Configuration C with operating airflow rates: 470 l/s (1000 cfm) from the ceiling inlet and 470 l/s (1000 cfm) from the door inlet.

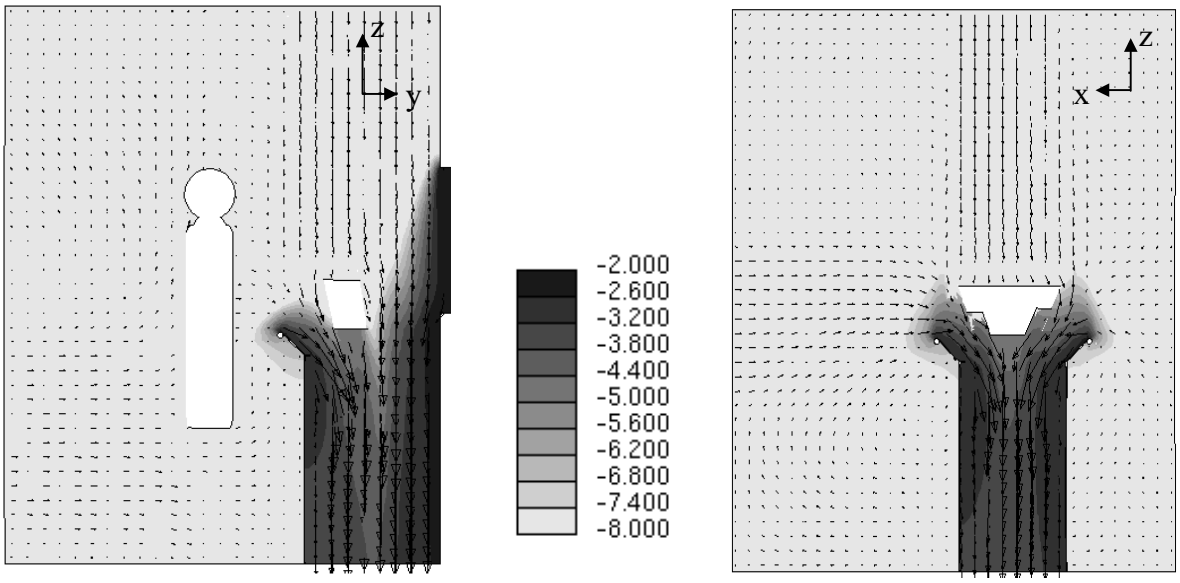

FIGURE 8. Velocity and tracer concentration with release of 1 g/s of tracer, Configuration E with operating airflow rates: 380 l/s (800 cfm) from the ceiling inlet, 280 l/s (600 cfm) from the door inlet, 70 l/s (150 cfm) from the airvest, 380 l/s (800 cfm) from the left side inlet and 140 l/s (300 cfm) from the right side inlet.

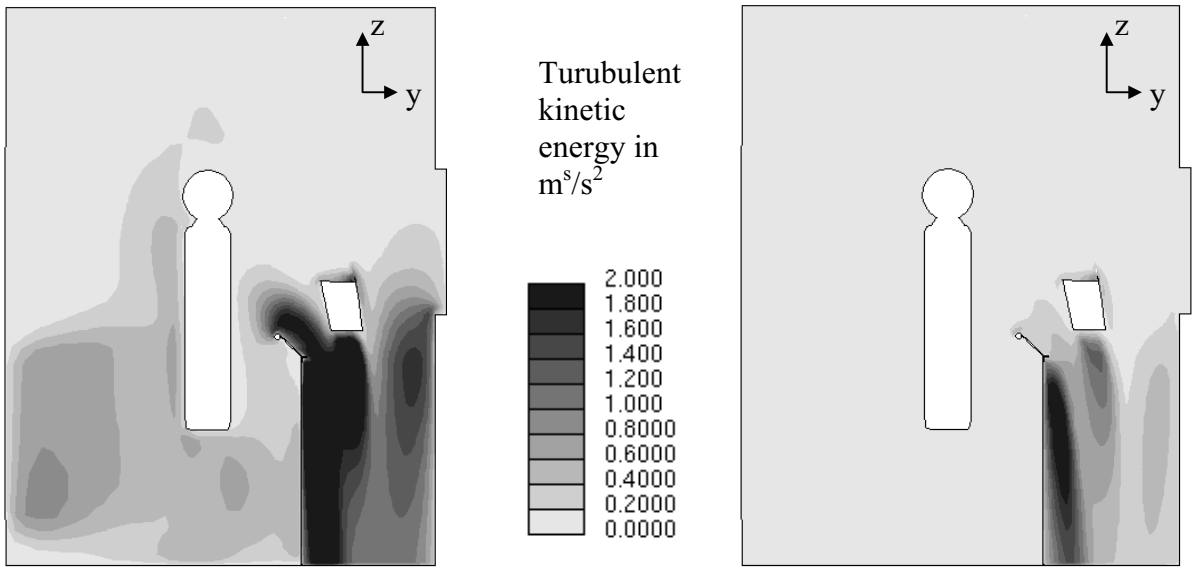

Figure 9. Turbulent kinetic energy for existing case (left) and for configuration E (right). Note dramatically lower turbulent kinetic energy throughout the room in Configuration E., which aids in improved containment.